Earth Systems, Resources, and Sustainability, 2026, 1(3), 265–281

Scilight

Earth Systems, Resources, and Sustainability

Journal Homepage: https://www.sciltp.com/journals/esrs

Article

Geochemical Characteristics of Tropical Estuarine Waters in Northern Borneo: Implication for Elemental Distribution, Mechanisms, Sources and Pollution Risk

Prasanna Mohan Viswanathan[1,*], Benedict Won Yong Tian[1], Chidambaram Sabarathinam[2] and Munirah Abdul Zali[3]

[1] Department of Applied Sciences, Faculty of Engineering and Science, Curtin University, Malaysia, Miri 98009, Sarawak, Malaysia
[2] Kuwait Institute for Scientific Research, P.O. Box 24885, Safat 13109, Kuwait
[3] Waste Technology and Environment Division, Malaysian Nuclear Agency, Bangi, Kajang 43000, Selangor, Malaysia
[*] Correspondence: prasanna@curtin.edu.my, ORCID - 0000-0002-9555-5337

ABSTRACT

Estuaries are exceptional and vital ecosystems which create a dynamic region with biological, ecological, and environmental advantages. In this study, surface water samples were collected at three estuaries (Miri River, Sibuti River and Kuala Baram River) adjoining the South China Sea, and compared with the upper section of the rivers. The collected samples were analysed for *in situ* parameters, major ions, trace metals and stable isotopes using standard procedures. Results showing spatial variations in ionic concentrations across three estuaries, controlled by multi-geochemical processes such as weathering, ion exchange and seawater influx. Dominant water types varied: Ca–Cl in Miri and Sibuti rivers, and Na–Cl in Kuala Baram River, indicating distinct influences of seawater mixing and ion exchange reactions. Evaporation process increased the salinity in estuaries, coupled with the anthropogenic impacts in the downstream. Ionic ratios also prove seawater and freshwater mixing, followed by mineral precipitation and ion exchange. The undersaturation state of carbonate and sulphate minerals indicates the dissolution in the lower and upper reaches of the rivers, and approaching towards saturation state in estuaries might lead to precipitation of minerals in favour of pH and seawater influx. The higher LogpCO_2 values in the upper sections of the rivers indicate the weathering of source rocks. The isotopic ratio of $\delta^{18}O$ and $\delta^{2}H$ and d-excess values confirm the progressive dominance of evaporation in estuaries due to the continental effect. Statistical analysis reveals key geochemical processes such as seawater mixing, weathering, ion exchange and anthropogenic activities, that impact the hydrochemistry of estuaries. Miri and Kuala Baram estuaries are at high and medium levels of pollution based on heavy metal evaluation index (HEI), which require continuous monitoring, particularly for the higher concentrations of Zn, Cu, Pb and Mn.

ARTICLE INFO

History:

Received 15 January 2026
Revised 3 March 2026
Accepted 11 March 2026
Published: 18 March 2026

Keywords:

estuary;
seawater mixing;
ion exchange;
evaporation;
Miri coast

Citation:

Viswanathan, P.V.; Tian, B.W.Y.; Sabarathinam, C.; et al. Geochemical Characteristics of Tropical Estuarine Waters in Northern Borneo: Implication for Elemental Distribution, Mechanisms, Sources and Pollution Risk. *Earth Systems, Resources, and Sustainability* **2026**, *1*(3), 265–281. https://doi.org/10.53941/esrs.2026.100016

Research Highlights

- Spatial variability of ionic distribution in tropical estuaries were studied.
- Ca–Cl and Na–Cl water types suggest seawater mixing, evaporation and ion exchange.
- Isotopes reveal progressive evaporation in estuaries due to continental effect.
- PCA determines seawater influx, weathering and anthropogenic impacts in estuaries.
- High to medium level of metal pollution in MRE and KBE needs continuous monitoring.

1. Introduction

Estuaries are dynamic ecosystems with a high degree of spatial and temporal discrepancy. Estuaries are important and productive ecosystems, which support ecologically and economically in terms of breeding ground for fish, human settlements and industrial activities [1–3]. Hence, estuaries are the sites of pollutant deposition from point and non-point sources from human settlement, industries, fishing-related activities, commercial shipping and other sources [4–6]. Metals in estuaries could alter dynamics of the environment and affect aquatic animal survival. Metals accumulate in the estuary's biosphere, contaminating the ecosystem from estuaries to oceans [7].

The estuary acts as an interactional zone between terrestrial and marine environments, providing diverse nutrients and metals from different sources; anthropogenic substances and natural runoff can later be deposited at the river mouth [4, 8]. The characteristics of metals and nutrients can be associated with the physical and chemical parameters of estuary water. The diffusion of metals and nutrients in estuaries is altered by the physical parameters such as temperature, pH level, and salinity of water, which could affect the marine life [5, 6]. The number of geochemical processes operating in the estuary, such as seawater mixing, ion exchange, weathering, mineral dissolution and evaporation, could decrease the water quality [3, 9, 10].

Several factors govern the temporal and spatial distribution of metals in the estuarine region. The studies on the metal concentrations in tropical regions reveal that the main sources of metals could be either natural or anthropogenic. The natural geochemical sources of metals in the estuary are governed by the physio-chemical condition of the water and the sediment or the riverine load into the estuary [3, 6]. The physio-chemical factors are mainly governed by pH, redox, temperature, DO and salinity [11]. These physico-chemical parameters are based on the riverine inputs, sediment water interaction and seasonal variation [12–14]. This process is also to a minor extent governed by biological transformation [15]. The biogeochemical reactions, such as the process of decomposition of organic matter in estuaries, especially with mangroves, influence metal partitioning [16].

The continuously growing population and fast development of urbanization and industrial settings in the Miri region lead to various pollutants from the activities contributing to the pollution of the dependent estuarine and coastal areas. Few studies were conducted in this region to evaluate the water and sediment quality of rivers. The metal occurrence and their distribution and sources in the Kuala Baram River were studied by earlier researchers [5]. Studies on Miri River water quality [9, 10] were focused on understanding the elemental composition and related geochemical processes. The recent study by Ref. [8] in the Miri River deals with the water quality in different size fractions and identifies the vulnerable zones of pollution. Ref. [6] studied the geochemical behaviour of water, sediments and suspended solids in the Sibuti River.

From the earlier studies, the individual river ecosystem has been concentrated with the limited focus on the estuaries. Hence, the present study is an integrated approach to understand the spatial variability of elemental concentrations using multiproxy data includes *in situ* parameters, major ions, nutrients, trace metals and isotopes in all the three major estuaries (Kuala Baram, Miri and Sibitu rivers) of the Miri coast. This study is the first attempt to compare the estuarine-scale elemental variability and identify the possible geochemical mechanisms controlling the water chemistry. This study also provides the cross-estuary pollution ranking based on the assessment of the pollution index.

2. Study Area

The study area encompasses three estuaries in the Miri coast, east Malaysia. The Miri city is located adjacent to South China Sea, between latitude of 4°3′20″ N to 4°3′45″ N and longitude of 113°50′30″ E to 113°50′50″ E in the (Figure 1). The three estuaries are the Kuala Baram (KRE) in the north, the Miri River (MRE) in the center, and the Sibuti River (SRE) in the south of the Miri coast. The climate variation in the Miri region is influenced by two monsoons; the North-East Monsoon has higher rainfall from October to March and the South-West Monsoon from May to September receives less rainfall (Parvin Raj and Prasanna, 2023). In terms of geology, sedimentary to metasedimentary rocks of Miocene and Quaternary alluvium cover the region [8]. During the sampling time (southwest monsoon), the average rainfall and temperature were recorded as 245.6 mm and 27 °C. The land use pattern of Miri includes agricultural land, which covers most of the region, residential areas in Miri City and the industrial estate in the north (close to the Kuala Baram estuary).

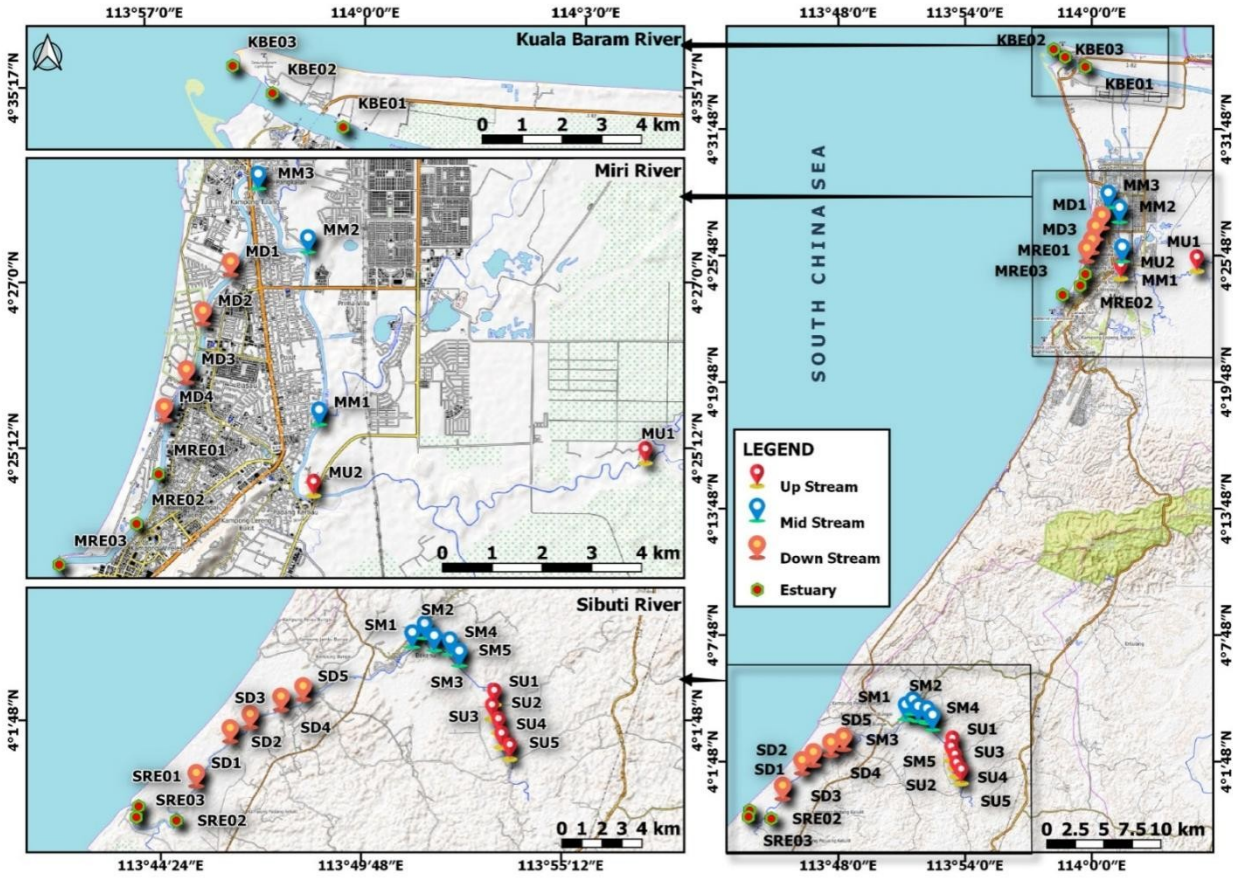

Figure 1. Study area map with the sample locations in all the three estuaries. Green circle with red dot indicates estuary samples, orange with white dot indicate downstream samples, blue with white dot indicate midstream samples and red with white dot represent upstream samples.

The Miri River extends for 45 km, and has a basin area of about 789.99 km^2, which is connected by numerous small river branches from the southeast of Miri, and ending at the Miri estuary towards the South China Sea [10]. The basin receives an annual rainfall of 2593–2750 mm, and the temperature ranges from 23 to 32 °C [3]. The geology of the river basin is covered by Neogene sediments, which consist of sandstone and shale alternations belonging to Miri Formation [17]. In terms of land use pattern, the upstream catchment is covered with palm plantations and urban settings in the downstream [8].

The Kuala Baram River is considered the second longest river in Sarawak State and occupies a catchment area of around 22,800 km^2. It releases an average of 1590 m^3/s of fresh water and 24 million tonnes of sediments into the sea [18]. Meta-sedimentary to sedimentary rocks of Paleogene and Recent alluvium are dominant in the river basin. It receives an annual rainfall of 2500–4000 mm. The major land use pattern in this basin is covered with primary, secondary and montane forests, with smaller portion of oil palm plantations, hill and wet paddy cultivation and mixed agricultural crops and fruit trees [19].

The Sibuti River is located 45 km southwest of Miri City, has a catchment area of 1020 km^2 and discharges into the South China Sea. The average annual rainfall and temperature at the river catchment are 3022 mm and 28.4 °C, respectively [6]. The river basin consists mostly of sedimentary rocks, ranging from Oligocene to Pliocene. The river is surrounded by mangrove forest and significant Bungai farm lands at the estuary, and agricultural activities in the upstream [20].

3. Methodology

3.1. Sample Collection and In Situ Measurements

In each estuary, 3 surface water samples (KBE, MRE and SRE) were collected at three different zones such as lower (river mouth), middle and upper (end of estuary) based on salinity variations, tidal influence and varying ionic concentrations (Figure 1). Samples were collected below 5 cm depth of the water surface and stored in 1L polyethylene bottles, and transferred to laboratory for further analysis by stored in a refrigerator at 4 °C to avoid contamination. The physical parameters such as temperature, pH, electrical conductivity (EC), total dissolved solids (TDS), salinity, turbidity and dissolved oxygen (DO) were measured *in situ* in each sampling point using portable meters with probes. For comparative study, hydrochemical data for the Miri River downstream (MRD), mid-stream (MRM) and upstream (MRU) were acquired from Ref. [21]; whereas for the Sibuti River downstream (SRD), mid-stream (SRM) and upstream (SRU) were acquired from

Ref. [6] by the same research team. For the Kuala Baram River, the only available downstream (KBD) data was acquired from Ref. [5]. The acquired secondary data has the identical season, analytical methods and detection limits as the analysed estuarine samples of this research. The only limitation of this comparative study is the unavailable dataset for the midstream and upstream of the Kuala Baram River. In addition, the temporal variability of elemental concentration is not focused in this study.

3.2. Lab Analysis

The collected samples were filtered using 0.45 µm filter paper for further chemical analysis. The nutrients, SO_4, NO_3 and PO_4 were analysed in the DR2800 Portable Spectrophotometer. Major ions, Cl and HCO_3 were analysed using titration [22], whereas Ca, Mg, Na and K were analysed using Flame Atomic Spectrophotometer. For the data validity, ionic balance error percentage calculation was carried out and it ranged within an acceptable $\pm$10% [23].

For the trace metals analysis, nitric acid was added to the samples and digested using a microwave digestor. Standards were prepared using available stock solutions and calibration curves were developed for the sample analysis. Finally, the trace metals such as Fe, Mn, Zn, Pb and Cu were analysed using a Flame Atomic Spectrophotometer. For the accuracy and the precision of results, cross-checking the measured samples against standards randomly.

Stable isotopes, $\delta^{18}O$ and $\delta^{2}H$ were analysed using isotope ratio mass spectrometry (FINNIGAN DELTAPLUS XP). The isotopic values were represented in parts per million (‰), and are defined as follows [24].

$$\delta(‰) = \left(\frac{R_{\text{sample}} - R_{\text{std}}}{R_{\text{std}}}\right) \times 10^3 \quad (1)$$

where, std refers to Standard Mean Ocean Water (*SMOW*), and R is defined as *D/H* or $^{18}O/^{16}O$.

3.3. Data Analysis

The chemical data were used to create geochemical plots and indices for further interpretation. Piper plot [25] and Gibbs diagram [26] were used to identify the water types, and the major geochemical processes impact the water chemistry. Geochemical model, WATEQ4F [27] was used to calculate the saturation state of carbonate and sulphate minerals, including LogpCO_2 and ionic strength. Statistical tool (SPSS version 17), principal component analysis (PCA) was used to determine the association of ions, and the underlying patterns with the identification of the responsible location for that process using factor score values [28]. The heavy metal evaluation index (HEI) was used to assess the overall pollution status of the estuaries with respect to the metal concentrations [29]. HEI is expressed as below.

$$\text{HEI} = \sum_{i=1}^{n}\left(\frac{H_c}{H_{\text{mac}}}\right) \quad (2)$$

where, H_c and H_{mac} refer to the measured value and maximum admissible concentration (MAC) of the ith parameter.

4. Results and Discussion

4.1. Hydrochemical Variations

The results of physico-chemical parameters in three estuarine waters along with the other sections of the rivers for comparison, are presented in Figures 2 and 3. The statistical results for the data are depicted in Table 1.

In KBE, pH ranged from 8.1 to 8.6, with an average value of 8.4, which is higher than the downstream (KBD) average pH, 6.8. This suggests the shifting of redox conditions from acidic to alkaline towards estuary. The higher average values of EC and TDS (47,713.7 µS/cm and 33,400 mg/L) than the average KBD value (3178.1 µS/cm and 1557.2 mg/L) were observed in the estuary waters. Similarly, the salinity was exponentially increased in the estuary (38.3 ppt), whereas the average KBD salinity was 1.64 ppt. It clearly indicates the influence of seawater mixing in the estuary waters [6, 30]. Higher DO values were observed in the estuary, ranging from 19.4 to 38.6 mg/L with an average of 30.6 mg/L, compared with the KBD's DO value (avg. 4.5 mg/L). Interestingly, turbidity was higher in the KBD samples, ranging from 45.5 to 284 NTU with an average of 114.78 NTU, whereas in the estuary, it was 44.5 NTU (average). It indicates intensive weathering and leaching of river bedrocks in the upstream, and subsequent sediment discharges into the downstream [5, 31]. The KBE waters have the following order of major ions: $Cl^- > Na^+ > Ca^{2+} > SO_4{}^{2-} > K^+ > Mg^{2+} > HCO_3{}^- > PO_4{}^{3-} > NO_3{}^-$. Whereas in KBD samples it follows as: $Cl^- > Na^+ > SO_4{}^{2-} > Mg^{2+} > K^+ > Ca^{2+} > HCO_3{}^- > PO_4{}^{3-} > NO_3{}^-$. Cl^- and Na^+ are dominant ions in both sections of the river. However, higher average values were observed in the KBD samples due to various processes/activities occurring in the lower Kuala Baram River [5]. In terms of trace metals, higher concentrations of Zn, Mn and Pb were observed in the estuary compared with the downstream section of the river. Interesting, Fe concentration was exponentially higher (avg. 4900 µg/L) downstream, as it was released from the source rocks of the river basin through chemical weathering [5, 8].

In the Miri River, temperature, pH, EC, TDS, DO, salinity and turbidity were higher in the estuary waters. It is also observed that an increasing trend of EC and TDS towards the estuary, considered as the receiving point of ionic concentrations. There is a clear increase in turbidity, DO and salinity observed in the estuary. The variation in pH (alkaline) and seawater mixing in the estuary could control the release and absorption of metal ions [8]. In terms of major ions, Cl^- and $SO_4{}^{2-}$ are the dominant ions in the estuary, whereas Cl^- and Na^+ in the lower and upper parts of the river. The sulfate enrichment in the estuary might be caused by the biochemical oxidation of reduced sulfur in the river sediments, coupled with the anthropogenic activities in the downstream [21, 32, 33]. The presence of sulfur in estuarine sediments of the Miri River, ranging

between 1.26 and 3.19% was reported by Ref. [34]. There was a drop in Ca^{2+}, Mg^{2+}, HCO_3^- and PO_4^{3-} concentrations in the estuary. Interestingly, NO_3^- concentration was detected in the estuarine waters. Fe and Mn showing the decreasing trend towards the estuary, indicating the formation of Fe-Mn oxyhydroxides as precipitate complexes in colloids and sediments, which was supported by higher pH and seawater influx [8, 35]. However, a sharp increase in concentration of Zn, Pb and Cu was observed in the estuary. The co-precipitation with Fe-OH and scavenging by other metals leads to higher levels of Zn, Pb and Cu in estuarine sediments, which later release into the water column based on the physico-chemical conditions [6, 36].

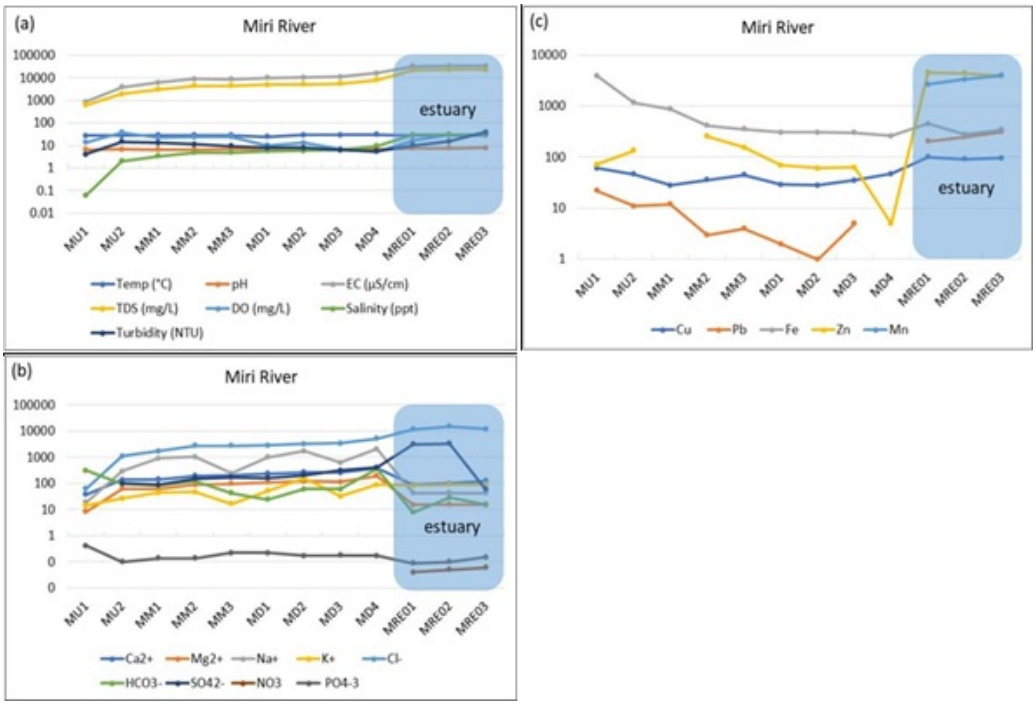

Figure 2. Spatial variations of elemental concentrations in the Miri River: (**a**) *in situ* parameters, (**b**) major ions, and (**c**) trace metals.

Figure 3. Spatial variations of elemental concentrations in the Miri River: (**a**) *in situ* parameters, (**b**) major ions, (**c**) trace metals, and Baram River: (**d**) physio-chemical parameters.

Table 1. Physico-chemical concentrations (range and average) in upstream, midstream, downstream and estuary sections of all the three rivers. All major ions and metals values are in mg/L.

	Range (mean)		Range (mean)				Range (mean)			
	Kuala Baram River		Miri River				Sibuti River			
Parameter	Estuary ($n = 3$)	Downstream ($n = 32$)	Estuary ($n = 3$)	Downstream ($n = 4$)	Midstream ($n = 3$)	Upstream ($n = 2$)	Estuary ($n = 3$)	Downstream ($n = 5$)	Midstream ($n = 5$)	Upstream ($n = 5$)
Temp (°C)	29.9–30.9 (30.4)	28.7–32.0 (30.1)	28.7–29.0 (28.9)	25.0-30.3 (28.7)	28.3–28.4 (28.3)	27.7–27.8 (28.2)	30.6–31.4 (31.1)	28.4–29.3 (28.8)	28–29.5 (28.7)	28.5–29.7 (29.3)
pH	8.12–8.58 (8.42)	4.6–7.5 (6.8)	7.6–7.9 (7.7)	6.9–7.0 (6.9)	6.67–6.89 (6.75)	6.58–6.66 (6.73)	7.4–7.7 (7.5)	5.9–6.3 (6.1)	6.1–6.4 (6.2)	6.3–6.5 (6.4)
EC (µS/cm)	39,285–54,428 (47,713.6)	39.5–9060.0 (3178.1)	32,285–33,857 (33,190)	10,120–16,220 (12,102.5)	6230–8950 (8016.6)	874–2364 (6496.3)	5942–24,485 (17,085)	163.5–301.3 (224.1)	134.3–216.5 (173.2)	145.2–176.9 (166.1)
TDS (mg/L)	27,500–38,100 (33,400)	19.0–4440.0 (1557.2)	22,600–23,700 (23,233.3)	5050–8110 (6045)	3100–4460 (3996.7)	612–1267.5 (3260.2)	4160–17,140 (11,960)	233.5–430.4 (320.1)	191.8–309.3 (247.4)	207.4–252.7 (237.3)
DO (mg/L)	19.4–38.6 (30.6)	0.4–5.6 (4.5)	16.7–30.6 (25.7)	5.3–13.1 (8.9)	22.4–24.6 (23.6)	13.9–25.8 (24.1)	22.5–35.2 (27.2)	4.1–4.6 (4.4)	4.3–6.4 (4.9)	4.56–4.77 (4.65)
Salinity (ppt)	27.5–50.1 (38.2)	0.0–5.1 (1.6)	29.3–30.9 (30.2)	5.6–9.5 (6.9)	3.35–4.95 (4.4)	0.06–1.04 (3.5)	4.6–21.5 (14.7)	1.13–1.19 (1.16)	0.03–1.16 (0.26)	0.020–0.030 (0.028)
Turbidity (NTU)	43.8–45.2 (44.5)	45.5–284.0 (114.7)	10.3–40.2 (21.9)	5.7–8.0 (7.0)	9.64–13.25 (11.42)	4.09–9.3 (10.9)	13.4–23.1 (17.5)	27.1–39.5 (34)	7.9–22.9 (19.3)	18.8–21.5 (19.7)
Ca^{2+}	11.81–44.17 (27.03)	0.4–301.0 (34.4)	89.5–125.8 (105.5)	234.0–390.0 (286.5)	142–210 (182)	38–89 (157.3)	41.4–88.3 (67.5)	2–4 (3.6)	2–4 (2.8)	4–6 (4.8)
Mg^{2+}	11.23–13.86 (12.87)	1.9–445.2 (77.3)	15.1–15.9 (15.5)	111.6–193.2 (135.3)	61.2–97.2 (82)	8.4–35.4 (69.65)	13.6–15.1 (14.5)	1.2–3.6 (1.9)	BDL-3.6 (1.9)	1.2–6 (3.6)
Na^{+}	36.97–42.07 (39.39)	2.6–1317.0 (377.0)	42.7–43.5 (43.0)	621.7–2058.0 (1355.1)	247.1–1053.1 (741.7)	19.1–155.08 (572.2)	40.8–43.3 (42.2)	46.4–128 (75.8)	26.8–80.6 (50.2)	27–74.4 (37.9)
K^{+}	6.73–22.72 (16.21)	1.6–279.2 (61.5)	83.4–92.0 (89.1)	32.8–161.3 (83.7)	16.6–48.0 (36.2)	14.4–20.6 (31.3)	22.2–84.1 (63.3)	9.8–17.7 (13.1)	9.6–20 (12.9)	8.9–20.4 (12.2)
Cl^{-}	177.25–354.5 (295.4)	BDL-2940.0 (966.6)	11,698.5–15,181.5 (13,087)	2898.0–5246.6 (3726.7)	1728.1–2747.3 (2401.7)	62.03–584.9 (1906.5)	2543.5–7444.5 (5781.3)	44.3–106.4 (70.9)	26.6–53.2 (40.8)	26.6–44.3 (37.2)
HCO_3^{-}	5.49–15.25 (8.9)	12.2–54.9 (27.7)	7.9–28.7 (17.3)	24.4–366.0 (128.1)	42.7–122 (83.3)	97.6–207.6 (114.2)	8.5–12.2 (9.8)	18.3–54.9 (35.4)	24.4–30.5 (28.1)	24.4–36.6 (32.9)
SO_4^{2-}	13–35 (23.6)	BDL-410.0 (131.1)	59–3300 (2153)	160.0–400.0 (270)	90–170 (136.6)	BDL-49 (113.08)	300–2800 (1733.3)	19–30 (23.2)	12–54 (35.4)	13–59 (35.6)
$NO_3^{-}N$	0.02–0.04 (0.03)	BDL-0.3 (0.04)	0.04–0.06 (0.05)	BDL	BDL	BDL	0.03–0.07 (0.05)	0.05–0.16 (0.10)	0.16–0.34 (0.25)	0.02–0.14 (0.08)
PO_4^{-3}	0.04–0.13 (0.07)	0.2–0.9 (0.2)	0.1–0.2 (0.1)	0.17–0.22 (0.19)	0.14–0.22 (0.16)	0.1–0.26 (0.19)	0.02–0.19 (0.12)	0.02–0.18 (0.07)	0.7–1.6 (0.9)	0.3–3.5 (1.7)
Cu	0.038–0.157 (0.109)	40–100 (60)	91–101 (95.7)	28–47 (34.8)	28–45 (36.3)	46–53.5 (40.6)	11–57 (30.7)	BDL	BDL	BDL
Pb	0.02–0.15 (0.109)	BDL-40 (10)	203–310 (253)	1–5 (2.7)	3–12 (6.3)	11–16.5 (9.16)	20–29 (24.5)	BDL	BDL	BDL
Fe	0.107–0.42 (0.25)	2300–10,800 (4900)	278–448 (356.3)	259–307 (292.5)	356–867 (545.3)	1159–2528 (1057.5)	219–297 (256.7)	2075–3075 (2485)	1775–2550 (2050)	1575–2050 (1730)
Zn	3.6–5.5 (4.2)	20–200 (40)	3903–4527 (4265)	5–69 (49.5)	156–256 (206)	71–102.5 (176.4)	950–3676 (2482.7)	121–164 (145.3)	130–165 (147.5)	103–169 (132)
Mn	0.90–2.79 (2.11)	60–100 (80)	2676–3984 (3331.3)	BDL	BDL	BDL	254–476 (342.3)	151–256 (182.4)	100–137 (125.4)	108–122 (114.6)

In the Sibuti River, there is a sharp increase in the levels of EC, TDS, and DO observed in the estuary, which facilitates redox processes by releasing metal ions [37]. pH and salinity were also increased to support the above mechanisms, including the seawater mixing. As in the Miri River, Cl^- and SO_4^{2-} are the dominant ions in the Sibuti estuary, whereas Cl^- and Na^+ are in the lower and upper parts of the river. Similarly, Ca^{2+}, Mg^{2+} and K^+ concentrations were increased in the estuary suggesting weathering and dissolution of cations through an ion-exchange process with the clay-dominant sediments [38]. NO_3^- showing a decreasing trend towards the estuary. Fe concentration showed a consistent trend in the downstream and upstream, then sharply decreased in the estuary as a result of salinity-induced flocculation [39]. However, Mn concentration was increased in the estuary. It suggests the adsorption-desorption process occurred in the varied redox conditions of the estuary. This process of metal exchange between sediment and the water column was observed to be significant in the estuary despite the absence of external sources [40]. Interestingly, Zn, Cu and Pb were only found in the estuary.

4.2. Geochemical Mechanisms

In the Piper plot (Figure 4), all the KB samples fall in the Na–Cl field, which indicates the salinization through seawater mixing [6]. However, the proportion of salinity varies with respect to the proximity of samples to the river mouth. For Miri River, MRD and MRM samples were clustered in the Na–Cl field, which suggests various anthropogenic activities dominated in the downstream [10]. A sample from MRU falls in Ca–Mg–HCO_3 indicates the weathering of source rocks [3]. Estuary samples were plotted in the Ca–Cl field. It is interesting to observe the hydrochemical evolutionary pathways from Na–Cl (downstream) to Ca–Cl (estuary). The observed changing cations from Na to Ca indicated the reverse ion exchange process, whereby Na^+ was observed in the estuary sediments and released Ca^{2+} into the water [5, 6]. This was supported by the calculated positive values of chloro-alkaline indices [41] for the samples. For the Sibuti River, SRU, SRM and SRD samples fall in the Na–Cl field, whereas the estuary samples were clustered in the Ca–Cl. The dominance of Cl^- in the estuary indicates the seawater influx and evaporation, which is a common mechanism in estuaries. Whereas, the Cl^- in other sections of the river is derived from various anthropogenic impacts [8, 10]. The shift of Na^+ to Ca^{2+} suggests a reverse ion exchange process.

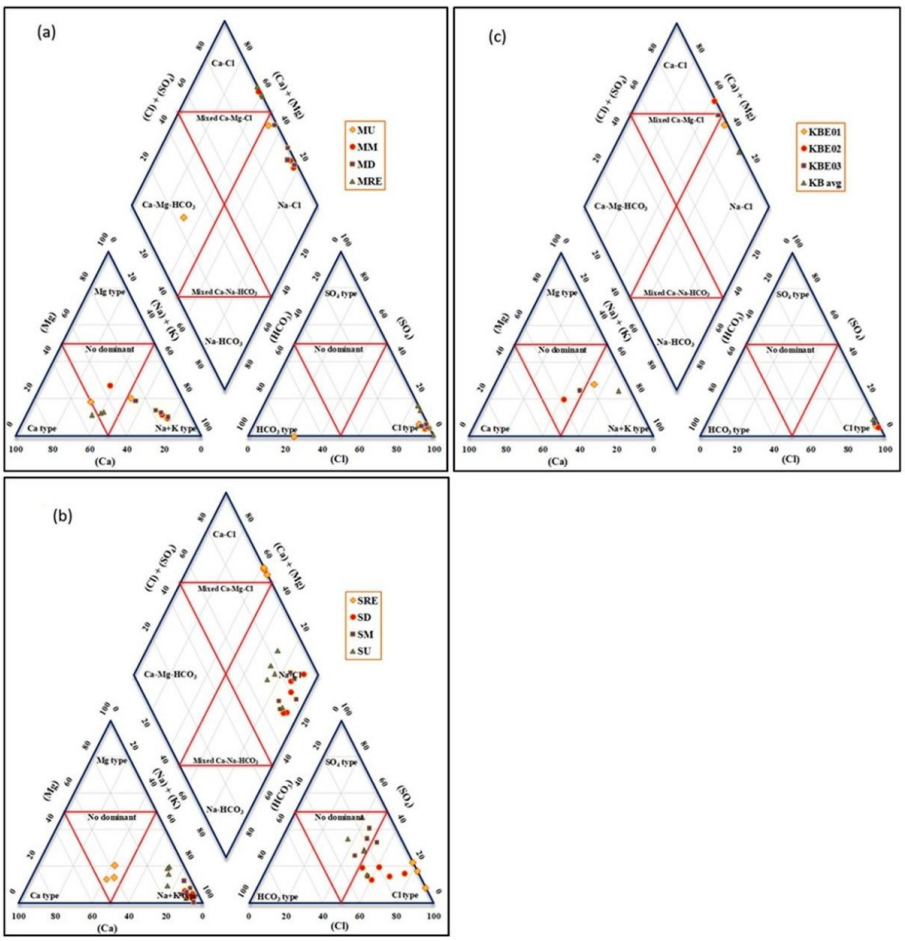

Figure 4. Piper plot to identify the water types and its hydrochemical evolutionary pathways in the three estuaries: (**a**) Miri River, (**b**) Sibuti River, and (**c**) Kuala Baram River.

In the Gibbs plot (Figure 5), KB estuary samples fall in the evaporation field, whereas the KBD sample falls outside the boomerang field. In the cation plot of the Miri River, samples from MRM and MRD fall within the evaporation dominance field, indicating natural surface evaporation with anthropogenic impacts [10]. The upstream samples fall close to the rock water interaction field suggest the weathering of source rocks in the river basin [8]. In the anion plot, all the samples fall close and in the evaporation field indicating the multiple sources of Cl^- from natural seawater influx and anthropogenic impacts [6, 10]. For the Sibuti River, most of the samples (except the estuary) fell outside the boomerang field, which indicates that the hydrochemistry of the estuaries water is impacted by other factors or anthropogenic activities like urban waste, agricultural run-off and industrial discharges. Estuary samples fall in the evaporation field, indicating the seawater mixing [6].

4.3. Ionic Ratios

In the present study, Cl^- is the most dominant anion in all rivers. This indicates the Cl^- might originate from the seawater mixed with the estuaries water, and other anthropogenic impacts [6, 30]. To explore the correlation between Cl^- and other cations, ionic ratio plots (Figure 6) were used to underscore the geochemical processes. In the Ca vs. Cl plot, the Sibuti River has a good positive correlation ($r^2 = 0.97$), particularly in estuarine samples (circled), with a higher ratio indicating the release of Ca^{2+} during reverse ion exchange with the increasing salinization suggests mixing of freshwater and seawater [42]. However, the Miri and Kuala Baram rivers show poor correlation. In SO_4 vs. Cl plot, all the 3 rivers show positive correlation, in which Kuala Baram and Sibuti Rivers are in good positive correlation ($r^2 = 0.98$; 0.93). The higher ratio in Miri and Sibuti estuaries indicates the release of sulfate from the sediments by the oxidation process, coupled with anthropogenic activities downstream. It was reported that the presence of sulfur in this estuarine sediment had an average of 2.13% in Miri estuary and 3.9% in Sibuti River [34]. There are no significant changes in the Na^+ concentrations in estuary waters indicating the loss of Na^+ from the solution during the mixing of seawater and freshwater. It is suggested that Na^{2+} in the seawater that invades the river water and is then depleted due to ion exchange during the recharge of water [43]. A similar trend was observed for Mg vs. Cl ratio. Thus, seawater influx is the potential source of hydrochemical alteration in the estuarine waters, followed by ion exchange and mineral precipitation.

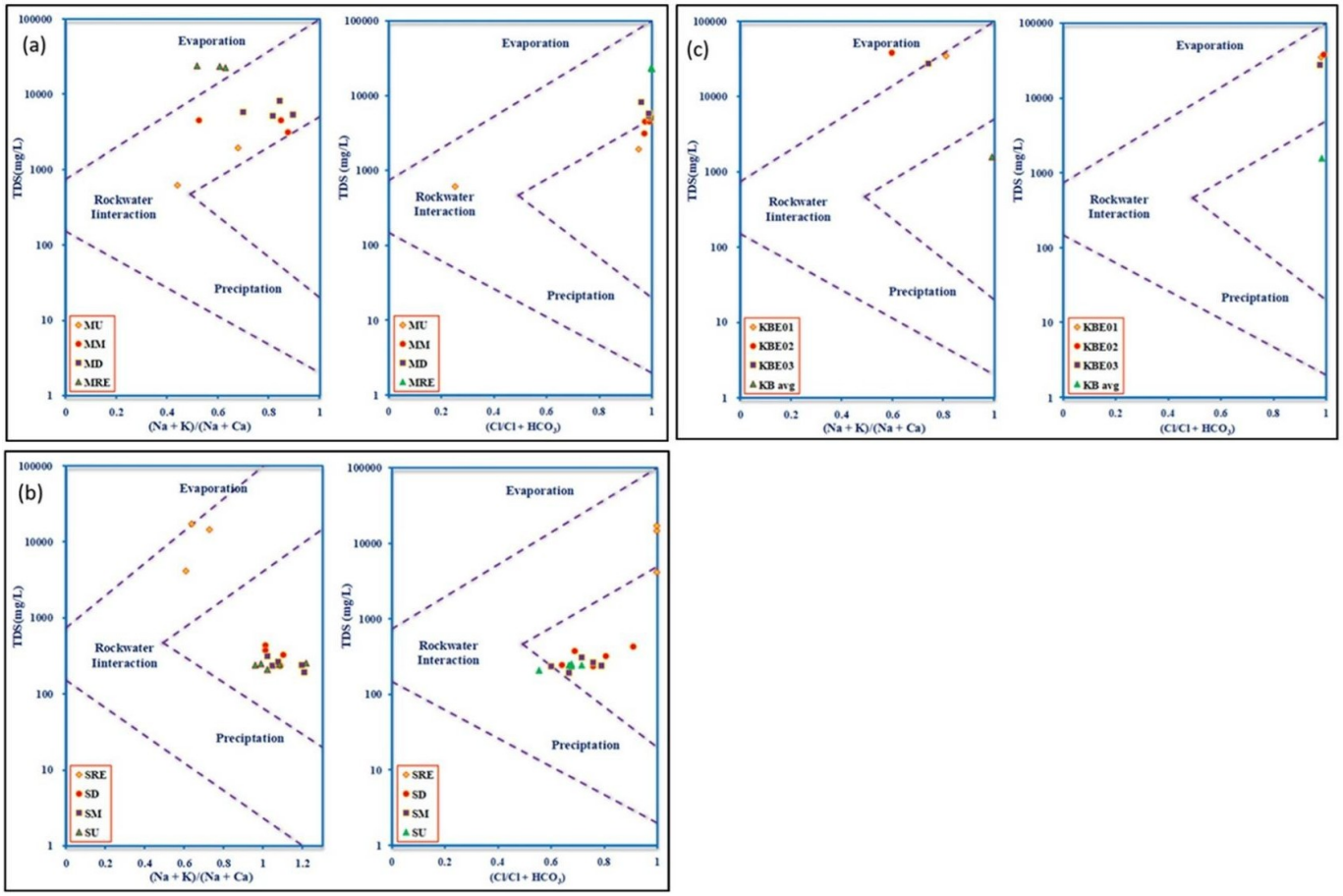

Figure 5. Gibbs plot to identify the major geochemical processes impact the estuarine water chemistry: (**a**) Miri River, (**b**) Sibuti River, and (**c**) Kuala Baram River.

4.4. Saturation Index (SI) and Log pCO_2

In order to determine the saturation state of minerals present in the estuarine waters, an attempt was made in this study to calculate the SI of carbonate and sulphate minerals (Figure 7). The SI values of carbonate and sulphate minerals indicate that all the samples fall under saturation state, which indicates dissolution of minerals from the river basin source rocks [21]. However, the increasing value of SI for calcite and aragonite in MRE and KBE might indicate an approach towards precipitation of minerals due to the variation in pH and seawater mixing [10]. Interestingly, in the Sibuti estuary, higher values of gypsum and anhydrite indicate the dominance of sulphate minerals as evaporites, and subsequent dissolution in the upper stream [6]. Overall, the increasing values in estuaries might promote the precipitation of minerals, whereas the dissolution of minerals (decreasing values) was observed in the lower and upper parts of the rivers.

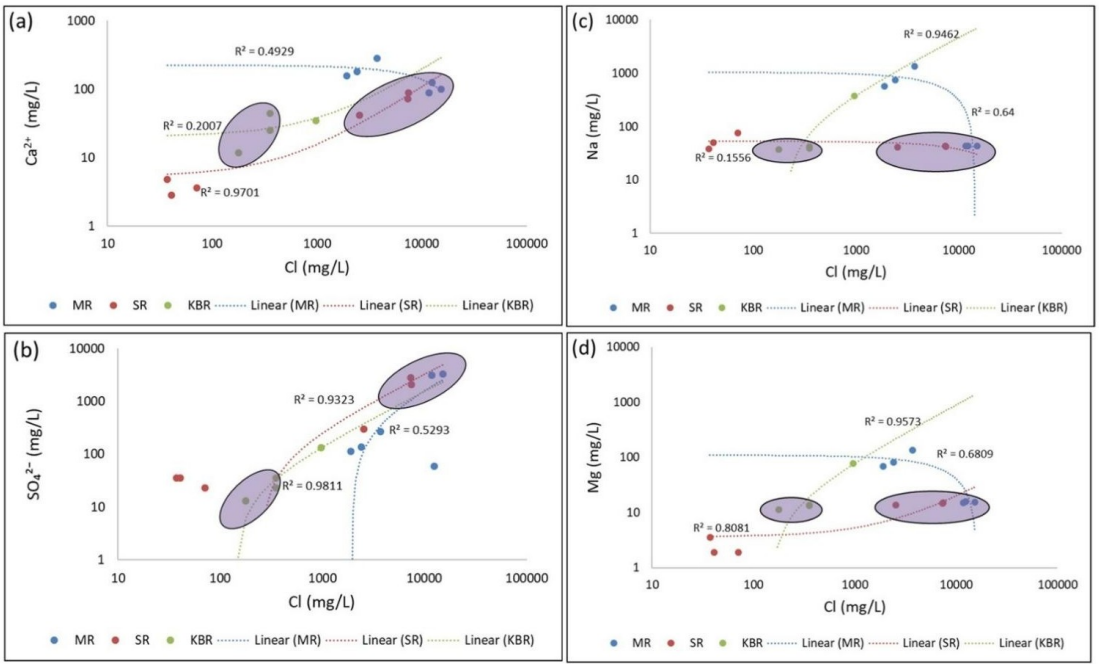

Figure 6. Ionic ratio to depicts Cl^- relationship with other ions, and its related geochemical controls: (**a**) Ca^{2+} vs. Cl^-, (**b**) SO_4^{2-} vs. Cl^-, (**c**) Na^+ vs. Cl^-, and (**d**) Mg^{2+} vs. Cl^-. Samples in the circles are estuarine samples.

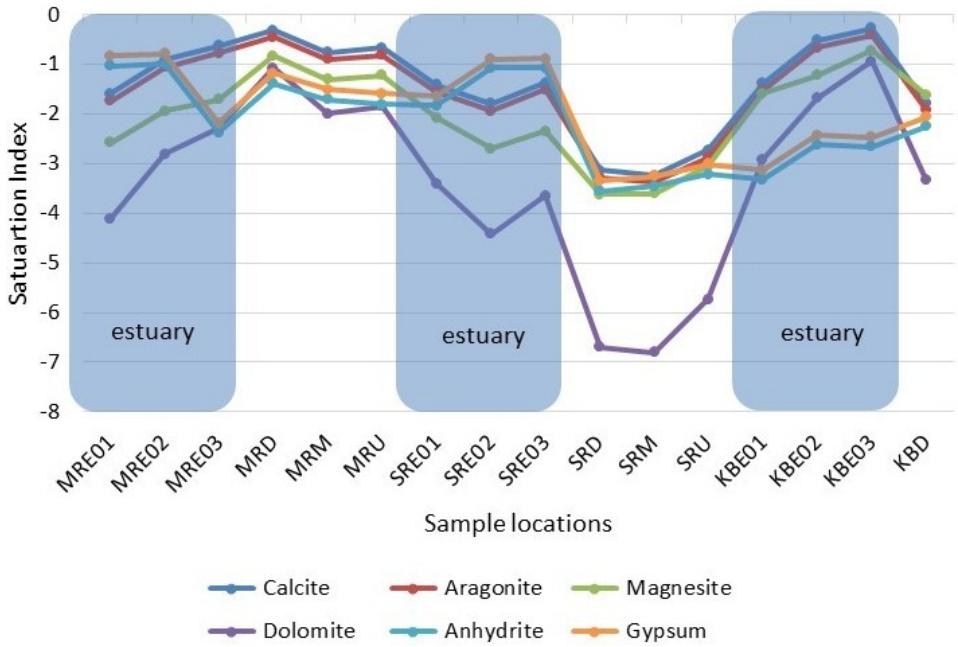

Figure 7. The calculated saturation index (SI) of carbonate and sulphate minerals present in the river waters. SI $= 0$ indicate equilibrium state, SI < 0 indicate undersaturation, and SI > 0 indicate oversaturation.

Log pCO_2 value is used to assess the residence time of water and its capacity for mineral dissolution in the environment [44]. Overall, estuarine samples were close to and above the atmospheric pCO_2 value (-3.5), which indicates the influence of precipitation source on the estuary water chemistry (Figure 8). However, there is an increasing trend of Log pCO_2 values were observed from KBE from the north to the SRE in the south with an increasing ionic strength. The higher Log pCO_2 values in downstream and upstream samples indicate that the waters are in extended contact with the river beds through weathering and dissolution of ions [6]. But the ionic strength was lower due to the dilution of ions, and carried towards the estuary.

4.5. Isotopic Signatures

In this study, the $\delta^{18}O$ values ranged from -9.79 to -3.64‰ with an average of -6.09‰ in MR; -11.20 to -9.54‰ with an average of -10.30‰ in SR; -9.91 to -8.80‰ with an average of -9.26‰ in KBR. Whereas, δ^2H ranged from -55.72 to -26.28‰ with an average of -38.34‰ in MR; -85.41 to -72.55‰ with an average of -78.61‰ in SR; -59.3 to -58.2‰ with an average of -58.63‰ in KBR. The enriched $\delta^{18}O$ and δ^2H values were observed in MR, whereas depleted values were observed in SR. The calculated d-excess values ranged from -6.19 to 22.6‰ with an average of 8.26 ‰. The higher d-excess values were observed in KBR and the lower values in SR.

$\delta^{18}O$ and δ^2H values were plotted in an X–Y scatter plot (Figure 9). In this study, the LMWL of the Limbang river basin is considered [28], as it has a similar tropical climatic pattern closer to the current study location. Similarly, GMWL is considered from Ref. [24]. In the $\delta^{18}O$ vs δ^2H plot, SR isotopic values were grouped in two different clusters. The cluster 1 samples from the lower part of the river (estuary and downstream) fall closer, and form a parallel relationship with GMWL and LMWL suggesting recharge through direct precipitation [21]. Whereas, cluster 2 samples from the upper part of the river (upstream and midstream) deviated away from LMWL/GMWL indicate evaporation [42]. Similarly, 2 clusters were identified for MR isotopic values. Cluster 1 from the lower part of the river consists of estuary and downstream samples that fall adjacent to the LMWL and GMWL indicate direct precipitation. However, it shows the enriched isotopic values due to the closest proximity to the ocean, and preferentially and the heavier ^{18}O is due to the continental effect [45, 46]. In this region, the air moisture originates predominantly from terrestrial source, particularly during the northeast monsoon which brings drier air masses leading to rainout effects [28, 47]. The cluster 2 samples are from the upper part of the river, which has depleted isotopic values, but slightly deviates from the LMWL. A slight increase (enriched) in $\delta^{18}O$ values were observed towards the river mouth sample (KBE01) in KBR, indicating the continental effect.

d-excess value was calculated using the equation, d-excess (‰) $= 8\delta^{18}O+10$ [48]. Most of the d-excess values for MR and KBR show high d-excess values (>10‰), which suggests the primary precipitation (Figure 10). However, it shows an evaporation trend towards the lower part of the river by the decreasing d-excess values, which again confirms the continental effect. The low d-excess values (<10‰) of SR indicate evaporation dominance [21]. The average d-excess value (8.2‰) of estuaries, which is deviated from the GMWL value (10‰), indicates that evaporation is the dominant process to control the hydrochemistry of rivers with lesser precipitation impact [49].

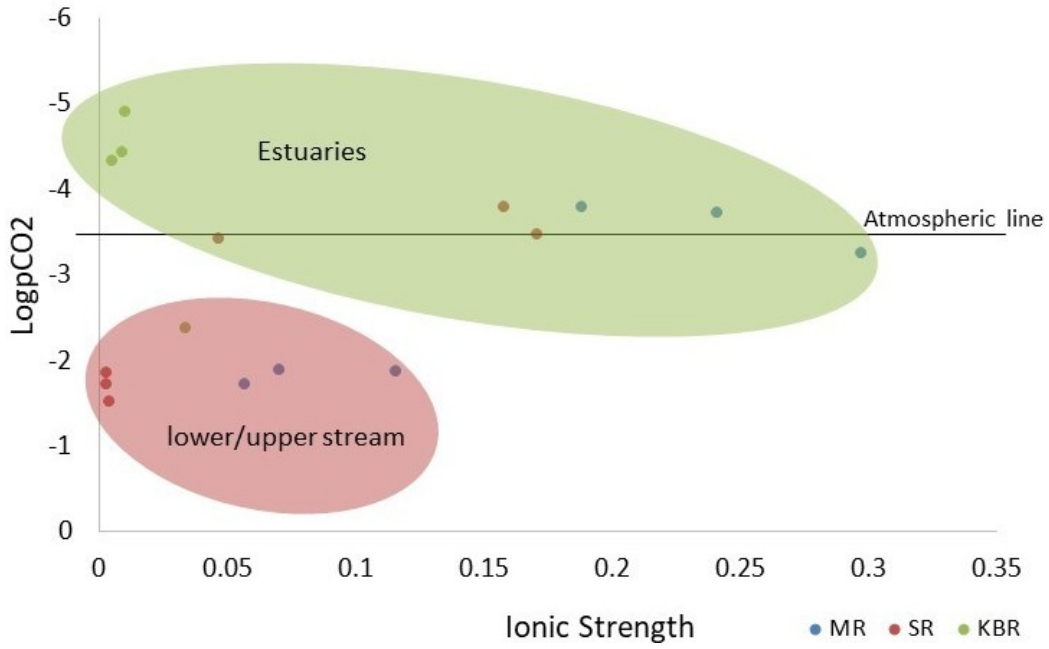

Figure 8. LogpCO_2 vs. ionic strength to understand the residence time of water in the river basin. The atmospheric Log pCO_2 value is -3.5.

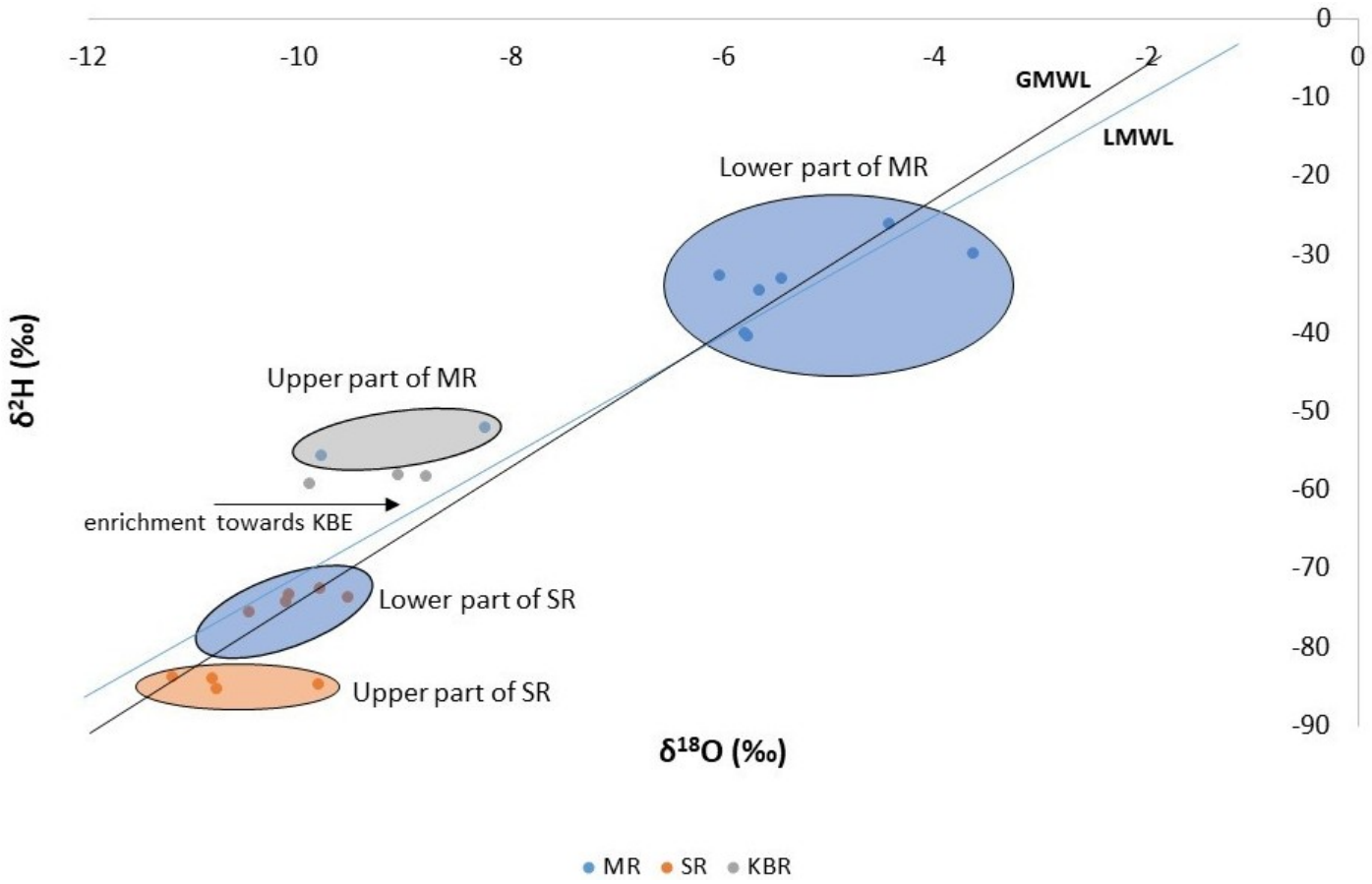

Figure 9. $\delta^{18}O$ vs. $\delta^{2}H$ plot to identify the various origins of water in the rivers. GMWL indicate global meteoric water line, and LMWL indicate local meteoric water line.

Cl concentrations were compared with $\delta^{18}O$ values to understand the salinization process in the rivers (Figure 11). An increasing value of $\delta^{18}O$ and Cl^- was observed from the upper to the lower part of MR indicating the evaporation dominance in the lower part of the rivers, which added salinization to the estuarine waters. Interestingly, SR showing large variance in Cl^- concentrations with constant $\delta^{18}O$ values signifies the evaporation dominance in the estuary. Similarly, KBE showing an increasing value towards the river mouth signifies the evaporation.

4.6. Principal Component Analysis (PCA)

The PCA extracted four factors with a total data variability of 85% (Supplementary Table S1). Factor 1 has loaded with pH, DO, EC, TDS and salinity, indicating the salinization process in all three estuaries [10]. Seawater mixing is the major potential source of hydrochemical alteration in the estuarine waters. The geochemical reactions in the buffer zone between the river water and seawater mixing also govern the elemental distribution in estuaries [35]. It is interesting to note that negative loading of metals indicates that salinity is also a prominant factor influencing the metal concentrations in estuarine waters [35, 50]. Factor 2 has loaded with Ca^{2+}, Mg^{2+}, Na^{+}, HCO_3^-, Cu and Pb suggests geogenic sources such as weathering, ion exchange and dissolution of minerals from the source rocks, present in the upper part of the Miri River [6, 18], which is reflected in the factor score (Figure 12). Factor 3 was loaded with K^{+}, Cl^- and SO_4^{2-} indicates oxidation of reduced sulfur in the river sediment releases SO_4^{2-} into water. The presence of sulfur mineral in the estuarine sediments, and the observation of sulphate mineral, gypsum ($CaSO_4$) in the dissolution state of saturation index, with the positive loading of Ca and SO_4 supported the above inference [32, 33]. This mechanism is mainly observed in the Miri and Sibuti estuaries, where the salinization by seawater mixing was reflected by Cl^- in this factor. Factor 4 was loaded with turbidity, and Fe suggests high sediment flow through river runoff. It was reported that the highest rate of sediment discharges occurred downstream of the Kuala Baram River [31]. This is mainly observed in the Kuala Baram estuary, which can support the above process. The sediment load derived from the terrestrial region, comprising of organic matter, clay, silt and sand mixture also influence the metal concentration in the region [15, 51]. Fe is mainly released from the chemical weathering of source rocks in the river basin [3]. The presence of colloids as a source of turbidity is higher in the estuary, which helps to carry Fe via adsorption [8].

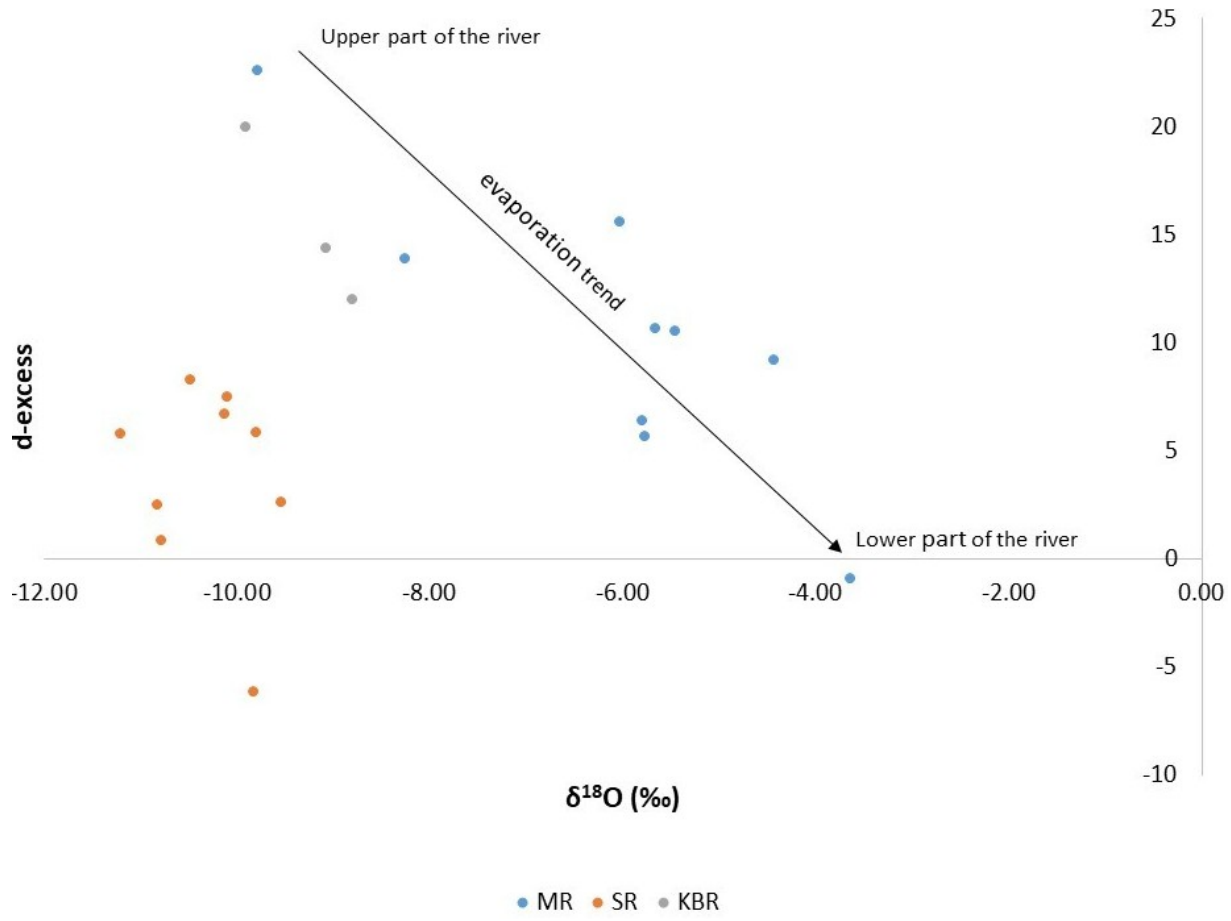

Figure 10. The calculated d-excess values were used to understand the evaporation and moisture sources of water in the rivers.

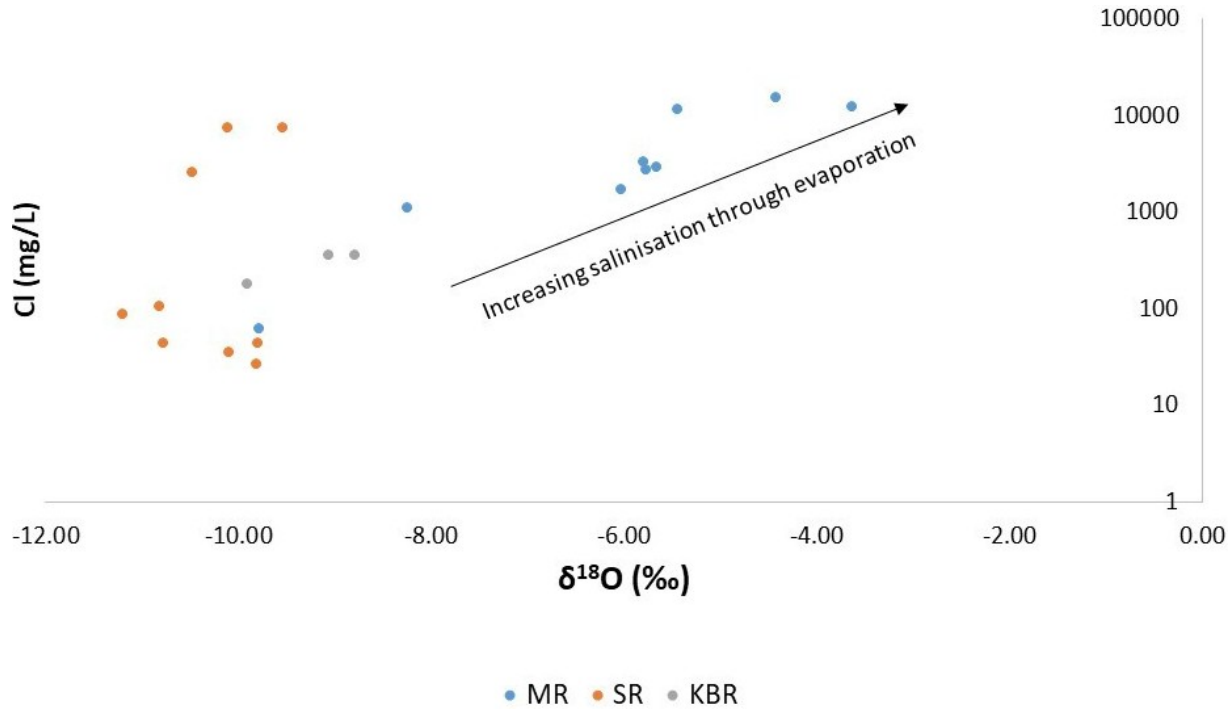

Figure 11. δ^{18}O vs. Cl plot to understand the salinization process in the estuarine waters.

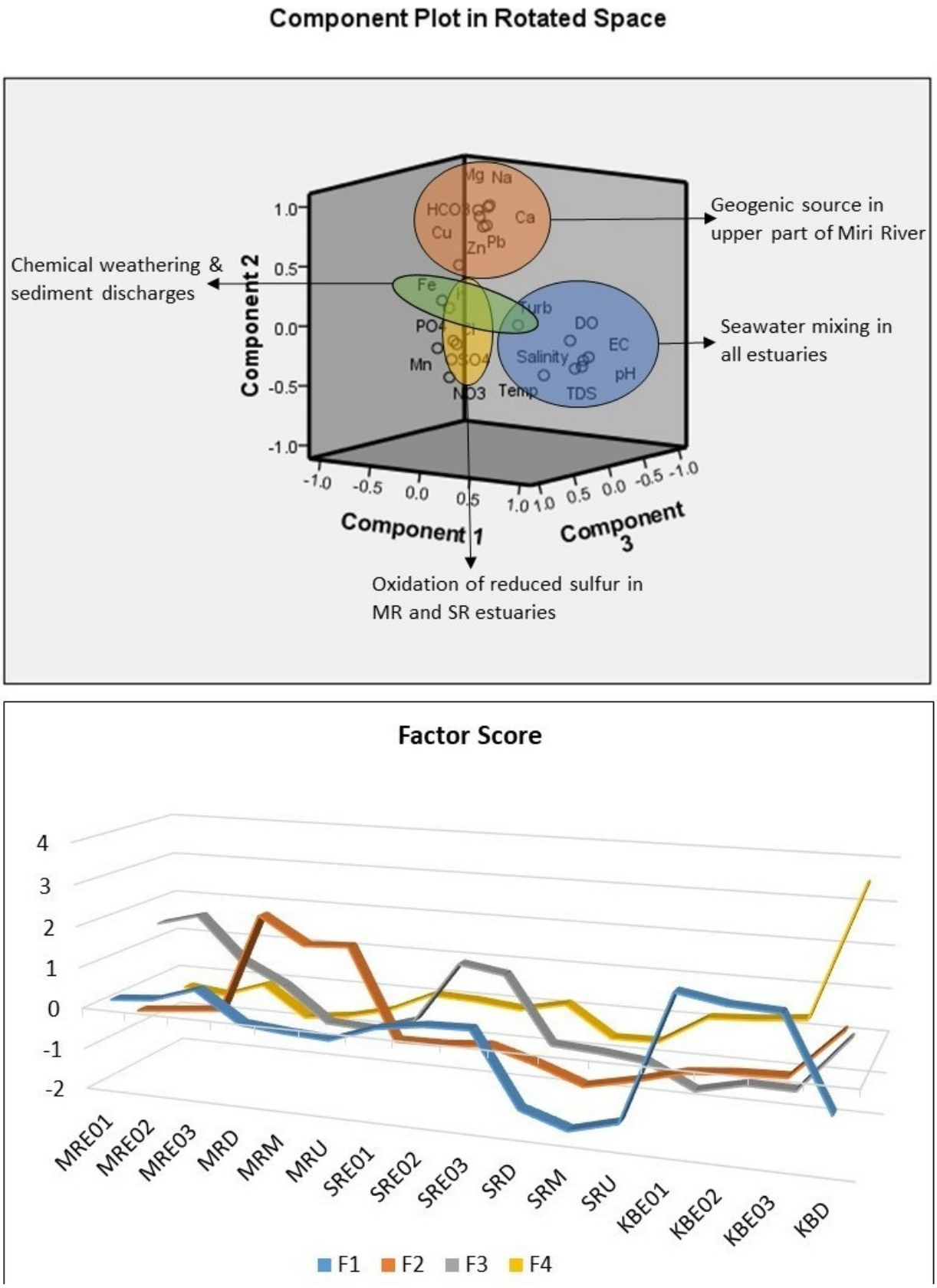

Figure 12. Principal component analysis for the hydrochemical data to identify the key geochemical processes that control the river water chemistry with respect to the site-specific as shown in the factor score plot.

4.7. Metal Pollution

Based on the Ministry of Health (MOH) Malaysia raw water quality standards, the concentration of Zn, Mn, and Pb in Miri and Kuala Baram estuaries exceed the guideline values. It is also observed that the Fe concentration in Sibuti upstream, mid-stream and downstream samples is higher than the MOH guideline values. The calculated HEI ranged from 1 to 28 with an average of 10. Based on the mean value of 10, three pollution categories were defined as low (>10), medium (10–20) and high (<20) [29]. Based on the classification, MR estuary samples fell in a high degree of pollution (Figure 13). Similarly, the majority of KB estuary samples fell in a medium degree of pollution. Whereas, SR samples fell in a low degree of pollution irrespective of the locations. The upper side of the rivers showing low pollution risk. Overall, the estuaries are vulnerable to metal pollution due to anthropogenic activities in the downstream that transport Zn, Cu, Pb, and Mn into the estuaries [5, 6]. In addition, the natural release of metals from the estuarine sediments due to varied redox conditions and salinity [39]. The benthic biodiversity has been reported to have declined due to the pollution load in the estuary [14]. The potential ecotoxicological risks to the estuarine organisms are particularly pronounced, especially in tropical regions, as tropical estuaries are rich in biota relative to other climatic regions [52–54]. Hence, this study shows that Miri coastal estuaries exhibit a higher to moderate risk of metal pollution, seeking attention with an effective periodic monitoring and management of the pollution sources.

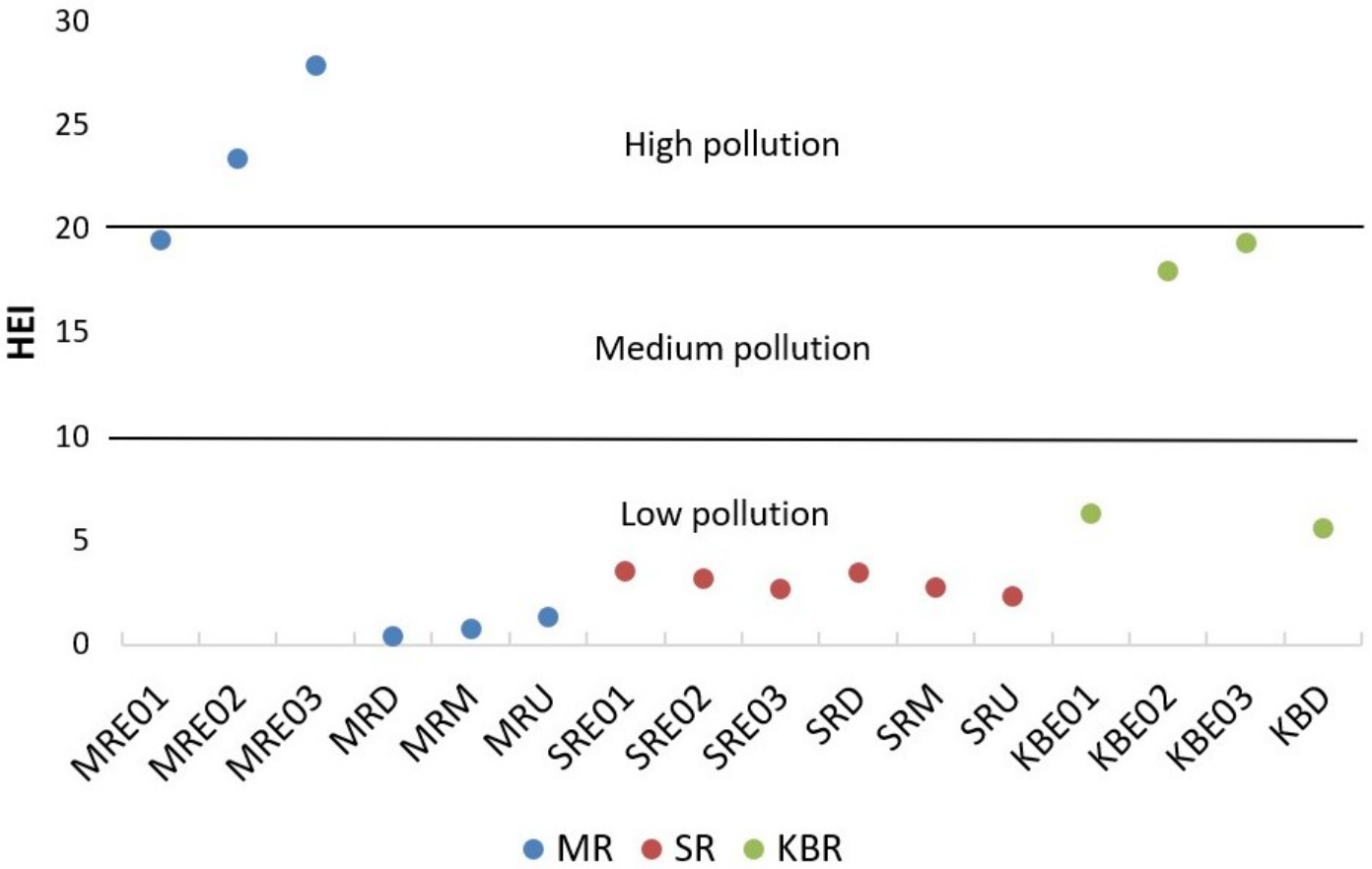

Figure 13. Heavy metal evaluation index (HEI) to identify the pollution status of the rivers. The samples were classified into three levels of pollution such as low, medium and high.

5. Conclusions

This study investigated regional estuarine-scale assessment by adopting multiproxy geochemical data to compare the elemental distribution, its processes and sources in three major estuaries of the Miri coast. Spatial variations of ionic concentrations showing distinct disparities among upper, lower and estuary sections of the rivers. Higher concentrations of EC, TDS, salinity, turbidity and TSS were observed in KBE, indicating seawater mixing into the estuary waters, with high sediment discharges through river runoff. Cl^- and SO_4^{2-} are the dominant ions in MRE and SRE, whereas Cl^- and Na^{2+} in KBE suggest the salinization and oxidation of reduced sulfur. Hydrochemical evolutionary pathway from Ca–Cl water type (MRE, SRE) to Na–Cl water type (KBE) indicates ion exchange and seawater influx. The upper section of the rivers has a Na–Cl water type indicate weathering and anthropogenic impacts. The dominance of surface water evaporation, seawater mixing and anthropogenic impacts is reflected in the Gibbs plot. Ionic ratio plots reveal that seawater mixing is the primary drivers of hydrochemical alteration in the estuarine waters. The undersaturation condition of carbonate and sulphate minerals suggests dissolution of minerals irrespective of rivers. However, the increasing SI values in estuaries might promote the precipitation of minerals under varying pH conditions. Estuaries Log pCO_2 values were close to the atmospheric value suggest the precipitation influence in the estuary waters. In contrast, the higher Log pCO_2 values in the upper sections indicate mineral weathering and dissolution. Isotopic signatures reveal primary precipitation in estuaries. However, d-excess values confirmed the evaporation dominance in estuaries with lesser precipitation influence due to the continental effect. PCA confirmed the dominance of seawater mixing in estuaries, and geogenic source influence in the upper sections of the rivers. The metal (Zn, Mn, and Pb) concentrations were higher than the MOH guideline values, particularly in Miri and Kuala Baram estuaries. Based on the pollution index (HEI), MRE and KBE were classified as high and medium degrees of metal pollution, with Zn, Cu, Pb and Mn as the most vulnerable metals in the estuaries. The outcome of this study reveals the current quality status of the estuaries in the Miri coast, which require continuous monitoring and sustainable management plans to protect this vulnerable ecosystem.

Supplementary Materials

The supporting information can be downloaded at: https://media.sciltp.com/articles/others/2603171628093795/ESRS-26010077-Supplementary_Materials.pdf.

Author Contributions

P.M.V.: Conceptualization; Data curation; Interpretation; Supervision; Writing original draft. B.W.Y.T.: Sample analysis. C.S.: Writing—review & editing. M.A.Z.: Isotopic analysis. All authors have read and agreed to submit to the journal.

Funding

This research received no external funding.

Institutional Review Board Statement

Not applicable.

Informed Consent Statement

Not applicable.

Data Availability Statement

All data used in this work are presented in the paper.

Acknowledgements

Authors thank to Faculty of Engineering and Science, Curtin University Malaysia for the support in lab analysis.

Conflicts of Interest

The authors declare that they have no known competing financial interests or personal relationships that could have appeared to influence the work reported in this paper.

Use of AI and AI-assisted Technologies

The authors have not used any AI tools for the preparation of the manuscript.

References

1. McLusky, DS.; Elliott, M. *The Estuarine Ecosystem: Ecology, Threats and Management*, 3rd ed.; Oxford University Press: Oxford, UK, 2004. https://doi.org/10.1093/acprof:oso/9780198525080.001.0001
2. Billah, M.; Kamal, A.; Hoque, M.; et al. Temporal distribution of water characteristics in the Miri estuary, east Malaysia. *Zool. Ecol.* **2016**, *26*, 134–140. https://doi.org/10.1080/21658005.2016.1148960
3. Nagarajan, R.; Eswaramoorthi, S.G.; Anandkumar, A.; et al. Geochemical fractionation, mobility of elements and environmental significance of surface sediments in a tropical river, Borneo. *Mar. Pollut. Bull.* **2023**, *192*, 115090. https://doi.org/10.1016/j.marpolbul.2023.115090
4. Saifullah, A.S.M.; Abu Hena, M.K.; Idris, M.H.; et al. Seasonal variation of water characteristics in Kuala Sibuti river estuary in Miri, Sarawak, Malaysia. *Malays. J. Sci.* **2014**, *33*, 9–22. https://doi.org/10.22452/mjs.vol33no1.3
5. Prabakaran, K.; Eswaramoorthi, S.; Nagarajan, R.; et al. Geochemical behaviour and risk assessment of trace elements in a tropical river, Northwest Borneo. *Chemosphere* **2020**, *252*, 126430. https://doi.org/10.1016/j.chemosphere.2020.126430
6. Rakesh Roshan, G.; Prasanna. MV.; Nagarajan. R.; et al. Spatial and temporal variations of geochemical processes and toxicity of water, sediments, and suspended solids in Sibuti River Estuary, NW Borneo. *Environ. Sci. Pollut. Res.* **2023**, *30*, 92692–92719. https://doi.org/10.1007/s11356-023-28596-5
7. Claridge, P.N.; Potter, I.C.; Hardisty, M.W. Seasonal changes in movements, abundance, size composition and diversity of the fish fauna of the severn estuary. *J. Mar. Biol. Assoc. U.K.* **1986**, *66*, 229–258. https://doi.org/10.1017/S002531540003976X
8. Fiona Bassy, W.; Prasanna, M.V.; Nagarajan, R.; et al. A comprehensive analysis of tracing the sources and dynamics of pollutants in a tropical Miri River, NW Borneo. *Sustain. Water Resour. Manag.* **2025**, *11*, 20. https://doi.org/10.1007/s40899-025-01203-w

9. Maharjan, A.K.; Wong, D.R.E.; Rubiyatno, R.; Level and distribution of heavy metals in Miri River, Malaysia. *Trop. Aquat. Soil. Pollut.* **2021**, *1*, 74–86. https://doi.org/10.53623/tasp.v1i2.20
10. Parvin Raj, S.R.; Prasanna, M.V. Occurrence and distribution of geochemical elements in Miri estuary, NW Borneo: Evaluating for processes, sources and pollution status. *Chemosphere* **2023**, *316*, 137838. https://doi.org/10.1016/j.chemosphere.2023.137838
11. Mondragón-Díaz, LF.; Molina, A.; Duque, G. Influence of environmental variables on the spatiotemporal dynamics of water quality in Buenaventura Bay, Colombian Pacific. *Environ. Monit. Assess.* **2022**, *194*, 720. https://doi.org/10.1007/s10661-022-10388-y
12. Dessai, D.V.G.; Nayak, G.N.; Basavaiah, N. Grain size, geochemistry, magnetic susceptibility: Proxies in identifying sources and factors controlling distribution of metals in a tropical estuary, India. *Estuar. Coast. Shelf Sci.* **2009**, *85*, 307–318. https://doi.org/10.1016/j.ecss.2009.08.020
13. Thanh-Nho, N.; Strady, E.; Nhu-Trang, T.T., et al. Trace metals partitioning between particulate and dissolved phases along a tropical mangrove estuary (Can Gio, Vietnam). *Chemosphere* **2018**, *196*, 311–322. https://doi.org/10.1016/j.chemosphere.2017.12.189
14. Akhtar, S.; Equeenuddin, S.M.; Roy, P.D. Spatial and seasonal variability of dissolved metals in a monsoonal estuarine environment. *Reg. Stud. Mar. Sci.* **2024**, *73*, 103463. https://doi.org/10.1016/j.rsma.2024.103463
15. Balachandran, K.K.; Laluraj, C.M.; Martin, G.D.; et al. Environmental analysis of heavy metal deposition in a flow-restricted tropical estuary and its adjacent shelf. *Environ. Forensics* **2006**, *7*, 345–351. https://doi.org/10.1080/15275920600996339
16. Amorim, R.M.; Delgado, J.de F.; Baptista Neto, J.A.; et al. The benthic macrofauna along the estuarine gradient of the Paranaguá estuary. *Reg. Stud. Mar. Sci.* **2020**, **39**, 101459. https://doi.org/10.1016/j.rsma.2020.101459
17. Liechti, P.; Roe, F.W.; Haile, N.S.; et al. *The Geology of Sarawak, Brunei and the Western Part of North Borneo*; Geological Survey Department, British Territories in Borneo, Bulletin 3; Geological Survey Department, British Territories in Borneo: Kuching, Sarawak, 1960; p. 360.
18. Nagarajan, R.; Armstrong-Altrin, J.S.; Kessler, F.L.; et al. Provenance and tectonic setting of Miocene siliciclastic sediments, Sibuti formation, northwestern Borneo. *Arab. J. Geosci.* **2015**, *8*, 8549–8565. https://doi.org/10.1007/s12517-015-1833-4
19. Vijith, H.; Dodge-Wan, D. Spatial and temporal characteristics of rainfall over a forested river basin in NW Borneo. *Meteorol. Atmos. Phys.* **2019**, *132*, 683–702. https://doi.org/10.1007/s00703-019-00714-4
20. Hoque, M.M.; Kamal, AH.; Idris, MH.; et al. Status of some fishery resources in a tropical mangrove estuary of Sarawak, Malaysia. *Mar. Biol. Res.* **2015**, *11*, 834–846. https://doi.org/10.1080/17451000.2015.101.6970
21. Fiona Bassy, W.; Prasanna, MV.; Nagarajan, R. Spatial and temporal distribution of geochemical elements and their processes in different size fractions–Miri River (NW Borneo). *Kuwait J. Sci.* **2024**. *51*, 100136. https://doi.org/10.1016/j.kjs.2023.10.004
22. APHA. *Standard Methods for the Examination of Water and Wastewater*, 19th Edition; American Public Health Association (APHA); American Water Works Association (AWWA); Water Environment Federation (WEF): Washington, DC, USA, 1998.
23. Freeze, A.R.; Cherry, J.A. *Groundwater*; Prentice-Hall, Inc: Englewood Cliffs, NJ, USA, 1979; p. 604.
24. Craig, H. Isotopic variation in meteoric water. *Science* **1961**, *133*, 1702–1703.
25. Piper, A.M. A graphic procedure in the geochemical interpretation of water analyses. *Eos Trans. Am. Geophys. Union* **1944**, *25*, 914–928. https://doi.org/10.1029/ TR025i006p00914
26. Gibbs, R. Mechanisms controlling world water chemistry. *Science* **1970**, *170*, 1088–1090. https://doi.org/10.1126/science.170.3962.1088
27. Ball, J.W.; Nordstrom, D.K. *User's Manual for WATEQ4F, with Revised Thermodynamic Data Base and Test Cases for Calculating Speciation of Major, Trace, and Redox Elements in Natural Waters*; U.S. Geological Survey Water-Resources Investigations Report 91-4183; U.S. Geological Survey (USGS): Denver, CO, USA, 1991; pp. 1–188.
28. Ninu Krishnan, M.V.; Prasanna, M.V.; Vijith, H. Isoscapes to address the regional precipitation trends in the equatorial region of southeast Asia. *Phys. Chem. Earth A/B/C* **2022**, *127*, 103159. https://doi.org/10.1016/j.pce.2022.103159
29. Edet, A.E.; Offiong, O.E. Evaluation of water quality pollution indices for heavy metal contamination monitoring. A study case from Akpabuyo-Odukpani area, Lower Cross River Basin (southeastern Nigeria). *GeoJournal* **2002**, *57*, 295–304. https://doi.org/10.1023/B:GEJO.0000007250.92458.de
30. Shin, K.; Koh, D.-C.; Jung, H. The hydrogeochemical characteristics of groundwater subjected to seawater intrusion in the archipelago, Korea. *Water* **2020**, *12*, 1542. https://doi.org/10.3390/w12061542
31. Collins, D.S.; Johnson, H.D.; Allison, P.A. Coupled 'storm-flood' depositional model: Application to the Miocene–Modern Baram Delta Province, north-west Borneo. *Sedimentology* **2017**, *64*, 1203–1235. https://doi.org/ 10.1111/sed.12316
32. Matson, E.A.; Brinson, M.M. Sulfate enrichments in estuarine waters of North Carolina. *Estuaries* **1985**, *8*, 279–289. https://doi.org/10.2307/1351488
33. Yin, H.; Hu X.; Dias, L.M. Sulfate enrichment in estuaries of the northwestern Gulf of Mexico: The potential effect of sulfide oxidation on carbonate chemistry under a changing climate. *Limnol. Oceanogr.* **2023**, *8*, 685–798. https://doi.org/10.1002%2Flol2.10335
34. Benedict Wong, Y.T. Geochemical Characteristics and Metals Dynamics in Estuaries of Miri Coastal Environment, Unpublished Bachelor's Thesis, Curtin University, Malaysia, 2024.
35. Zhao, G.; Ye, S.; Yuan, H. Surface sediment properties and heavy metal pollution assessment in the Pearl River Estuary, China. *Environ. Sci. Pollut. Res.* **2017**, *24*, 2966–2979. https://doi.org/10.1007/s11356-016-8003-4
36. Essien, J.P.; Antai, S.P.; Olajire, A.A. Distribution, seasonal variations and ecotoxicological significance of heavy metals in sediments of cross river estuary mangrove swamp. *Water Air Soil Pollut.* **2009**, *197*, 91–105. https://doi.org/10.1007/s11270-008-9793-x
37. Taghavi, S.M.; Nasrabadi, T.; Kachoueiyan, F. Effect of oxidation-reduction potential on flocculation and mobility of metals in an estuarine environment. *Reg. Stud. Mar. Sci.* **2025**, *89*, 104278. https://doi.org/10.1016/j.rsma.2025.104278
38. Oyuntsetseg, D.; Ganchimeg, D.; Minjigmaa, A. Isotopic and chemiocal studies of hot and cold springs in western part of Khangai Mounbtain region, Mongolia for geothermal exploration. *Geothermics* **2015**, *53*, 488–497. https://doi.org/10.1016/j.geothermics.2014.08.010
39. Omar, T.F.T.; Aris, A.Z.; Yusoff, F.M. Occurrence, distribution, and sources of emerging organic contaminants in tropical coastal sediments of anthropogenically impacted Klang River estuary, Malaysia. *Mar. Pollut. Bull.* **2018**, *131*, 284–293. https://doi.org/10.1016/j.marpolbul.2018.04.019
40. Vipindas, P.V.; Anas, A.; Jayalakshmy, K.V. Impact of seasonal changes in nutrient loading on distribution and activity of nitrifiers in a tropical estuary. *Cont. Shelf Res.* **2018**, *154*, 37–45. https://doi.org/10.1016/j.csr.2018.01.003
41. Scholeller, H. Qualitative evaluation of groundwater resources. In *Methods and Techniques of Groundwater Investigations and Development*; UNESCO: Paris, France, 1965; pp. 54–83.
42. Al Farrah, N.; Walraevens, K. Hydrogeological and hydrogeochemical investigation of the coastal area of Jifarah Plain, NW Libya. *Afr. Focus* **2011**, *24*. 95–99. https://doi.org/10.21825/af.v24i1.18029
43. Gopinath, S.; Srinivasamoorthy, K.; Saravanan, K. Tracing groundwater salinization using geochemical and isotopic signature in Southeastern coastal Tamilnadu, India. *Chemosphere* **2019**, *236*,

124305. https://doi.org/10.1016/j.chemosphere.2019.07.036

44. Stephan, O.; Prasanna, M.V.; Anshuman, M. A multiproxy analysis of rainwater chemistry and moisture sources in Borneo. *Earth Syst. Environ.* **2025**, *9*, 3271–3288. https://doi.org/10.1007/s41748-025-00653-8
45. Rozanski, K.; Araguas-Araguas, L.; Gonfiantini, R. Isotopic patterns in modern global precipitation. In *Climate Change in Continental Isotopic Records*; American Geophysical Union Monograph, Volume 78; American Geophysical Union (AGU): Washington, DC, USA, 1993; pp. 1–36.
46. Winnick, M.J.; Chamberlain, C.P.; Caves, J.K. Quantifying the isotopic 'continental effect'. *Earth Planet. Sci. Lett.* **2014**, *406*, 123–133.
47. Aggarwal, P.; Gibson, J.J.; Froehlich, K.; et al. Isotopic evidence for climatic conditions on southeast Asia at the last glacial maximum. In *Conference: Study of Environmental Change using Isotope Techniques, Vienna, Austria*; IAEA C&S Papers Series 13/P; IAEA: Vienna, Austria, 1993; pp. 28–40.
48. Dansgaard, W. Stable isotopes in precipitation. *Tellus* **1964**, *16*, 436–468.
49. Zheng, L.; Jiang, C.; Chen, X. Combining hydrochemistry and hydrogen and oxygen stable isotopes to reveal the influence of human activities on surface water quality in Chaohu Lake Basin. *J. Environ. Manag.* **2022**, *312*, 114933. https://doi.org/10.1016/j.jenvman.2022.114933
50. Shilla, D.J.; Tsuchiya, M.; Shilla, D.A. Terrigenous nutrient and organic matter in a subtropical river estuary, Okinawa, Japan: Origin, distribution and pattern across the estuarine salinity gradient. *Chem. Ecol.* **2011**, *27*, 523–542. https://doi.org/10.1080/02757540.2011.600831
51. Akita, L.G.; Laudien, J.; Nyarko, E. Geochemical contamination in the Densu Estuary, Gulf of Guinea, Ghana. *Environ. Sci. Pollut. Res.* **2020**, *27*, 42530–42555. https://doi.org/10.1007/s11356-020-10035-4
52. Tang, Z.; Liu, X.; Niu, X. Ecological risk assessment of aquatic organisms induced by heavy metals in the estuarine waters of the Pearl River. *Sci. Rep.* **2023**, *13*, 9145. https://doi.org/10.1038/s41598-023-35798-x
53. Sultan, M.B.; Anik, A.H.; Rahman, Md.M. Emerging contaminants and their potential impacts on estuarine ecosystems: Are we are of it? *Mar. Pollut. Bull.* **2024**, *199*, 115982. https://doi.org/10.1016/j.marpolbul.2023.115982
54. Basraoui, N-e.; Ben-tahar, R.; Deliege, J-F. Potentially toxic elements contamination and ecological risk assessment in surface sediments of Moulouya Estuary (Northeastern, Morocco). *Sci. Afr.* **2024**, *24*, e02295. https://doi.org/10.1016/j.sciaf.2024.e02295